As proposed, we continued to investigate the physical basis of semi-empirical laws for rate and state friction. Work presented at the 2004 and 2005 SCEC meetings provided enough information to warrant further investigation of evolution laws and the importance of evolution laws to the healing of faults in interseismic periods. We made significant progress. We have published 3 papers in G^3 [1,2,3]. Our paper on pure compaction has been accepted by *JGR* [4]. Our salient overall contribution demonstrates the thermodynamic bases of semi-empirical friction relationships from laboratory studies. This augments confidence in exporting these relationships to physical representation of real faults in the Earth's crust. Fault mechanics including rupture initiation and field observation of faults are significant parts of the current SCEC effort by several investigators.

Evolution laws. We begin with evolution laws of rate and state friction that represent the transition between static and sliding friction. For brevity and because we plan application to diffuse strain away from faults, we present the strain-rate rather than the velocity form of the relationships [5,6]. In terms of macroscopic variables, the fault zone width is W, shear strain rate is the ratio of velocity to fault zone thickness $\varepsilon' \equiv V/W$, and reference strain rate is proportional to a reference velocity $\varepsilon'_0 \equiv V_0/W$. The instantaneous shear traction is

$$\tau = P\left[\mu_0 + a\ln(\varepsilon'/\varepsilon'_0) + b\ln(\psi/\psi_{\text{norm}})\right], \quad (1)$$

where P is normal traction (effective pressure in general although we present drained case for simplicity), μ_0 is the coefficient of friction at reference conditions, a and b are small dimensionless constants. The inverse of the state variable ψ represents damage. The normalizing value for the state variable is

$$\psi_{\text{norm}} = P^{\alpha/b}/P_0^{\alpha/b}, \quad (2)$$

where α is a small dimensionless parameter than represents the behavior of the surface after a change in normal traction from [7], and P_0 is a reference normal traction. The static-stress earthquake triggering is expected wherever the Coulomb stress change $\Delta\tau/\Delta P$ exceeds the critical value differential coefficient of friction $\partial\tau/\partial P = \mu_0 - \alpha$ where the strain rate change is zero at constant state.

The state variable evolves with time. In the formalism, its value depends on the past history of damage from sliding. Various forms of evolution laws have been proposed. In the notation of [5, 6], the Dieterich [8] or aging evolution law is

$$\frac{\partial\psi}{\partial t} = \frac{\varepsilon'_0 P^{\alpha/b}}{\varepsilon_{\text{int}} P_0^{\alpha/b}} - \frac{\psi\varepsilon'}{\varepsilon_{\text{int}}}. \quad (3)$$

the intrinsic strain $\varepsilon_{\text{int}} \equiv D_c/W$ (where D_c is the critical displacement), The first right-hand term represents healing and the second term damage from sliding. It has the properties that the state variable increases with time (linearly for constant normal traction) when sliding is stopped during a hold.

The Ruina [9] or slip evolution law in our notation is

$$\frac{\partial\psi}{\partial t} = -\frac{\varepsilon'\psi}{\varepsilon_{\text{int}}}\ln\left[\frac{P_0^{\alpha/b}\varepsilon'\psi}{P^{\alpha/b}\varepsilon'_0}\right], \quad (4)$$

The aging and slip laws make similar predictions if the velocity slows down (or speeds up) by less than a factor of e. (Andrew Ruina and Jim Dieterich prefer that the

descriptive names be used.) The evolution laws become increasingly different for more severe slow-downs. In the limit of a "hold" $\varepsilon' = 0$, the aging law predicts that the state variable increases linearly with time, while the slip law predicts no change. That is, with the slip law, the state variable at the time that pre-seismic creep commenced would be its value in the immediate aftermath of the last earthquake. It is irksome that the aging law seems to work better sometimes and the slip law others. For example, the aging law prevails for simulated gouge under humid conditions and the slip law under dry conditions [10] (See [1,2,11] for more discussion.)

Both laws evolution become compaction laws when we apply the Segall and Rice [12] relationship between porosity f and the state variable:

$$\psi = \exp\left(\frac{\phi - f}{C_\varepsilon}\right), \quad (5)$$

where ϕ is a reference porosity and C_ε is a dimensionless material property. The aging and slip evolution equations for porosity then become

$$f' = \frac{C_\varepsilon \varepsilon'}{\varepsilon_{\text{int}}} - \frac{C_\varepsilon \varepsilon'_0 P^{\alpha/b}}{\psi \varepsilon_{\text{int}} P_0^{\alpha/b}} \quad (6); \qquad f' = \varepsilon' \frac{C_\varepsilon}{\varepsilon_{\text{int}}} \left[\ln\left(\frac{\varepsilon'}{\varepsilon'_0}\right) + \ln\left(\frac{\psi}{\psi_{\text{norm}}}\right) \right], \quad (7)$$

It is generally agreed that friction on a molecular level is thermally activated exponential creep [13-17]. In terms of microscopic quantities within a contact asperity,

$$e'_{ij} = \frac{\gamma' \tau_{ij}}{r} \exp\left[\frac{r}{s}\right], \quad (8)$$

where e' is the strain rate tensor, ij are tensor indices, γ' is a constant with dimensions of strain rate, τ_{ij} is the deviatoric stress tensor, s is a material constant with dimensions of stress, and the second invariant r is $\sqrt{\tau_{ij}\tau_{ij}}$ normalized without loss of generality so that it is the shear traction in simple shear.

We used the productive approach of expressing the invariant in (8) in terms of the net stresses over the contact, which may scale with macroscopic quantities. That is, $r^2 \propto \tau^2 + c^2 P^2$, in macroscopic terms [1]. We constructed finite difference models to model exponential flow within a contact [2]. This yields parametric equations for strain rates [2,18, eqns. 20 and 22]. With some mathematics including Taylor series expansionss, we obtained the slip law with the following assumptions: the microscopic stresses at the contact scale to the macroscopic ones, the creep rate depends exponentially on the microscopic stress invariant r, and that the fault zone dilates at a rate proportional to the shear strain. These assumptions yield the feature that no strengthening or compaction occurs during a hold. Conversely, the aging law (6) arises when these assumptions do not apply. Particularly when different asperities accommodate shear traction and shear strain and normal traction and compaction strain. This may occur within a heterogeneous material where hydrated material at real contacts facilitates shear [8, 18-20] and compaction occurs elsewhere. It has applies to pure compaction where the normal traction dominates the stress invariant. This situation is likely persist where rock bears lithostatic load in many off-fault environments. We are currently applying the aging load to healing of rock damage in the shallow subsurface resulting from strong seismic waves and to the related effect of nonlinear attenuation of strong waves.

The stability parameter $a - b$ determines whether a fault can become unstable. Our work [2] on asperities between two sliding sheets shows that this parameter depends on

the shape of the asperities. For example, rectangular contacts formed at the expense of 2-D triangular prisms imply that this parameter is zero. We have not yet obtained a relationship between the stability parameter and fractal properties of a surface or gouge.

We obtained the porosity state relationship in (5) as the first term in a Taylor series relating real contact area to porosity. However, a simple explanation for the effect of sudden changes of normal traction on friction does not arise. Equation (2) is thus only a useful empirical approximation.

Frictional dilatancy. We assumed that the rate of dilatant frictional strain is a constant fraction of shear strain when we derived the slip law in [1,2]. We presented a simple derivation of this assumption in [3] in terms of measurable physical parameters. As a practical matter, dilatancy reduces the fluid pressure within an undrained fault zone. This effect increases friction and tends to quench earthquakes.

Overall we found it productive to consider gouge [1], sliding surfaces [2, 3], and compacting rock [4]. The relationship between frictional strain and damage is evident on a sliding surface. We present a brief version of our derivation in [3]. We start with the well-known derivation for the constant coefficient of friction μ_0, the leading term in (1). Failure (for example in quartz) occurs with the real shear traction of the order of 5-10 GPa from indenter data from [21]. The quantity is large enough compared to s in (8) to warrant approximating the flow law with failure at a shear yield stress τ_y. A yield stress for normal traction P_y arises similarly. The effects of macroscopic shear and normal traction both act on an asperity and effect the stress invariant τ within the asperity so there is an implicit geometrical assumption about the contact, which we have investigated in the current proposal to derive the slip evolution law [1,2].

In the traditional contact-theory derivation, microscopic properties scale to the macroscopic ones, the coefficient of friction

$$\mu_0 \equiv \frac{\tau}{P} = \frac{\tau_y}{P_y} \quad . \quad (9)$$

The derivation to this point is well known. We extend it to include anelastic strains within regions overrun by contact asperities. We apply the dimensional result that the real shear and normal tractions are comparable and that they scale with macroscopic properties.

We include elasticity with the justification that an infinitely rigid material stores no elastic strain energy. We justify ignoring inertia in [3]. We follow the effects of the normal traction P as we give dimensional results. That is, we do not distinguish at this stage between τ and P, whose ratio is the order of 1. We initially let the shear modulus G dimensionally represent the elastic modulus for the actual geometry. We implicitly apply Saint-Venant's principle [*22*, pages 89-90] throughout the discussion, the difference between loading by asperities and uniform loading by the macroscopic stresses away from the asperity being examined does not matter.

We consider friction between two surfaces to avoid the geometrical complexity of gouge. That is, we associate the separation rate of the plates with dilatancy in gouge. We follow the path of a representative asperity of radius A. For bookkeeping purposes, the asperity stays attached to the "upper" sheet in the figure. The lower sheet is initially planar and parallel to the upper sheet. The contact bears the macroscopic stresses over a region of radius R. That is

$$\pi A^2 P_y = \pi R^2 P \quad . (10)$$

The asperity crosses a surface area of the lower "substrate" sheet of $2AVt$ over time t. The yield stresses act on the base of the asperity, causing the immediate substrate to yield downward to a depth scaling with the radius A. The volume of damaged substrate produced over the time is dimensionally $VA^2 t$.

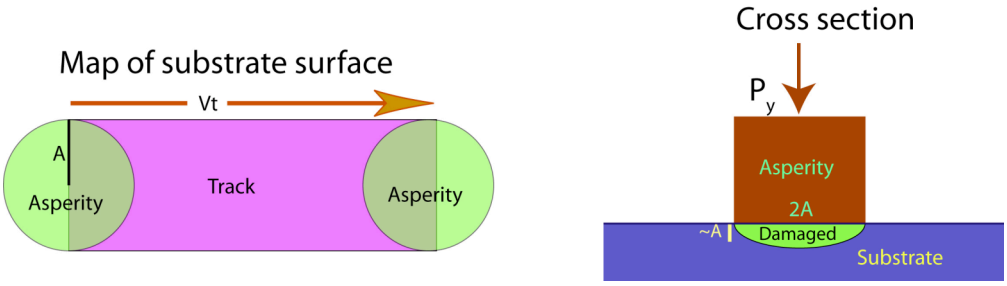

Stresses in the substrate change as the asperity moves. The aftermath of its passage on the lower sheet is relevant. For simplicity, consider that the asperity slides on a planar surface parallel to the sheets. The "flat" position of the deformed material exposed after the passage of the asperity is that with the asperity on it with normal traction P_y. With the load of the asperity removed, the exposed substrate material springs back, but stresses remain. The deformation is comparable to that from a negative normal traction scaling to P_y over the exposed area. We use this feature as a statistical average to obtain macroscopic scaling relationships for dilatancy. In general, deforming and object beyond its elastic limit leaves residual stresses and strains comparable to those at the yield criterion in its wake.

Beginning with microscopic energies, the elastic strain energy per volume in the region damaged by passage of the asperity scales as $N = P_y^2 / G$, assuming that the stresses within the damaged region are comparable to the yield stress. The rate that the moving asperity creates elastic strain energy is dimensionally

$$Q = VA^2 N = \frac{VA^2 P_y^2}{G} = \frac{VR^2 P_y P}{G} \quad . (11)$$

We assume that comparable fractions of the available energy go into local elastic strains and work against normal traction (dilatancy). That is, the total energy Q dimensionally represents both the local strain energy and the energy associated with dilatancy. We now equate microscopic and macroscopic effects to obtain the final equality from (10) which gives the macroscopic production rate of elastic energy, which is independent of the asperity radius. We compare this rate with the rate of dissipation of energy over this area from macroscopic friction, which is

$$Q_f = VR^2 \mu P \quad . (12)$$

This yields that the ratio of elastic strain energy production to frictional energy dissipation scales (the dilatancy coefficient β) as

$$\frac{Q}{Q_f} \approx \frac{P_y}{G} \approx \frac{\tau_y}{G} \approx \beta \quad , (13)$$

where the coefficient of friction μ is set to 1 because we have already dropped other factors of this order in our dimensional presentation. Final approximate equality is useful as it involves only shear parameters. We do not distinguish this energy result $\mu_0 P V_z = \beta \tau V_x$ from the kinematic statement in (6) $V_z = \beta V_x$ that the dilatational velocity (or strain rate) is proportional to the shear velocity. With more care in [3], the dilatancy coefficient is a large fraction of $\tau_y / 2G$ or ~5% for quartz. The measured dilatancy coefficient is ~4%, in agreement. Our work shows need to include elasticity in contact theory.

Nonlinear attenuation and rock damage by strong seismic waves. We have begun to study nonlinear attenuation of strong seismic waves [e.g., 22-26] and transient changes in S-wave velocity following strong shaking [e.g., 27-31]. The two phenomena are related effects of rock damage. They occur in the shallow subsurface, upper 100 m in soft rocks, mathematically above a depth of ~1/4 wavelength where the ratio of dynamic to lithostatic stress is highest. The energy required to open cracks to reduce S-wave velocity against lithostatic stress is a significant source of attenuation of the incident strong wave. This result agrees with direct measurement of significant nonlinear attenuation of strong seismic waves in soft rocks [23].

S-velocity velocity changes are easily and commonly observed in low-velocity rock. Inconveniently, trivial S-wave velocity changes may be associated with significant attenuation of strong waves within hard rock. Shear cracks may dissipate significant energy but they do not efficiently generate porosity. Nonlinear attenuation and S-wave delays occur over a broad range of dynamic stress. We infer that this implies that failure occurs within small domains with high pre-stress and with dynamic stress concentrations, rather than a single yield stress expected from naïve friction. The aging law (3) readily explains the tendency for S-wave delays to recover with the logarithm of time after strong shaking. The analysis also implies that much of the porosity change occurs in small domains, rather than as a small uniform change throughout the rock.

Quantifying nonlinear attenuation will aid in understanding how empirical relationships between shaking and earthquake distance arise. Nonlinear attenuation is both a site effect from the impinging wave and a regional effect in basins where reverberating waves attenuate each time they reflect from the free surface. Overall it limits the maximum particle velocity and dynamic stress at the surface. Understanding of its physical bases will aid in including the effect in representations of strong ground motions. Dynamic and kinematic modeling of earthquake ruptures and the seismic waves generated by them are major efforts in the SCEC project by many investigators.

[1] Sleep, N. H. (2005), Physical basis of evolution laws for rate and state friction, *Geochem. Geophys. Geosyst.*, *6*, Q11008, doi:10.1029/2005GC000991. *SCEC contribution number 896.*

[2] Sleep, N. H. (2006), Real contacts and evolution laws for rate and state friction, *Geochem. Geophys. Geosyst.*, *7*, Q08012, doi:10.1029/2005GC001187. *SCEC contribution number 991.*

[3] Sleep, N. H. (2006), Frictional dilatancy, *Geochem. Geophys. Geosyst.*, *7*, Q10008, doi:10.1029/2006GC001374. *SCEC contribution number 1030.*

[4] Hagin, P., N. H. Sleep, and M. D. Zoback (2005), Application of rate-and-state friction laws to creep compaction of unconsolidated sand under hydrostatic loading conditions, revision submitted to *J. Geophys. Res.*

[5] Sleep, N. H., E. Richardson, and C. Marone (2000) Physics of strain localization in synthetic fault gouge, *J. Geophys. Res*., *105*(B11), 25,875-25,890.

[6] Sleep, N. H. (1997), Application of a unified rate and state friction theory to the mechanics of fault zones with strain localization, *J. Geophys. Res*., *102*(B2) 2875-2895.

[7] Linker, M. F., and J. H. Dieterich (1992), Effects of variable normal traction on rock friction: Observations and constitutive equations, *J. Geophys. Res.*, *97*(B4), 4923-4940.

[8] Dieterich, J. H. (1979), Modeling of rock friction: 1. Experimental results and constitutive equations, *J. Geophys. Res*., *84*(B5), 2161-2168.

[9] Ruina, A. (1983), Slip instability and state variable laws, *J. Geophys. Res*, *88*(B12), 10,359-10,370.

[10] Frye, K. M., and C. Marone (2002), The effect of humidity on granular friction at room temperature, *J. Geophys. Res.*, *107*(B7), 2309, doi:10.1029/2001JB00654.

[11] Boettcher, M. S., and C. Marone (2004), Effects of normal stress variation on the strength and stability of creeping faults, *J. Geophys. Res*., *109*(B3), B033406, doi: 10:1029/2003JB002824.

[12] Segall, P., and J.R. Rice (1995), Dilatancy, compaction, and slip-instability of a fluid-penetrated fault, *J. Geophys. Res.*, *100*(B11) , 22,155-22,171.

[13] Rice, J. R., N. Lapusta, and K. Ranjith (2001), Rate and state dependent friction and the stability of sliding between deformable solids, *J. Mech. Phys. Solids*, *49*(9), 1865-1898.

[14] Nakatani, M. (2001), Conceptual and physical clarification of rate and state friction: Frictional sliding as a thermally activated rheology, *J. Geophys. Res.*, *106*(B7)), 13,347-13,380.

[15] Beeler, N. M. (2004), Review of the physical basis of laboratory-derived relations for brittle failure and their implications for earthquake occurrence and earthquake nucleation, Pure Appl. Geophys., 161(9-10), 1853-1876.

[16] Berthoud, P., T. Baumberger, C. G'Sell, and J.-M. Hiver (1999), Physical analysis of the state- and rate-dependent friction law:: Static friction, Phys. Rev. B., 59(22), 14,313-14,327.

[17] Nakatani, M., and C. Scholz (2004), Frictional healing of quartz gouge under hydrothermal conditions: 2. Quantitative interpretation with a physical model, *J. Geophys. Res*., *109*(B7), B07202, doi: 1029/2003JB002938.

[18] Anthony, J. L., and C. Marone (2005), The effect of humidity and granular particle dimension on the frictional properties of simulated fault gouge, *J. Geophys. Res., 110*(B8), B08409, doi: 10.1029/2004JB003399.

[19] Hong, T. and C. Marone (2005), Effects of normal stress perturbations on the frictional properties of simulated faults, *Geochem. Geophys. Geosystems, 6*, Q03012, doi:10.1029/2004GC000821.

[20] Di Toro, G., D. L. Goldsby, T. E. Tullis, (2004), Friction falls toward zero in quartz rock as slip velocity approaches seismic rates, Nature, 427(6973), 436-439.

[21] Goldsby, D. L., A. Rar, G. M. Pharr, and T. E. Tullis, (2004), Nanoindentation creep of quartz, with implications for rate- and state-variable friction laws relevant to earthquakes mechanics, *J. Mater. Res.*, *19*(1), 357-365.

[22] Sokolnikoff, I. S., (1956), *Mathematical Theory of Elasticity*, McGraw-Hill, New York, 476 pp.

[23] Beresnev, I. A. (2002) Nonlinearity at California generic soil sites from modeling recent strong-motion data, *Bull. Seismol. Soc. A., 92*, 863-870.

[24] Bonilla, L. F., R. J. Archuletta, and D. Lavallée (2005) Hysteretic and dilatant behavior of cohesionless soils and their effects on nonlinear site response: Field data observations and modeling, *Bull. Seismol. Soc. A., 95*, 2373-2395.

[25] Tsuda, K., J. Steidl, R. Archuleta, and D. Assimaki (2006) Site-response estimation for the 2003 Miyagi-Oki earthquake sequence consider nonlinear site response, *Bull. Seismol. Soc. Am., 96*, 1474-1482.

[26] Tsuda, K., R. J. Archulete, and K. Koketsu (2006) Quantifying the spatial distribution of site response by use of the Yokohama high-density strong-motion network, *Bull. Seismol. Soc. Am., 96*, 926-942.

[27] Rubinstein, J. L., and G. C. Beroza (2004), Nonlinear strong ground motion in the M_L 5.4 Chattenden earthquake: Evidence that preexisting damage increases susceptibility to further damage, *Geophys. Res. Lett., 31*, L23614, doi:10.1029/2004GL021357.

[27] Rubinstein, J. L., and G. C. Beroza (2004), Evidence for widespread nonlinear strong motion in the M_W 6.9 Loma Prieta Earthquake, *Bull. Seismol. Soc. Am., 94*, 1595-1608.

[29] Rubinstein, J. L., and G. C. Beroza (2005), Depth constraints on nonlinear strong ground motion from the 2004 Parkfield earthquake, *Geophys. Res. Lett., 32*, L14313, doi:10.1029/2005GL023189.

[30] Sawazaki, K., H. Sato, H. Nakahara, and T. Mishimura (2006), Temporal change in site response caused by earthquake strong motion as revealed from coda spectral ratio measurement, *Geophys. Res. Lett, 33*, L21303, doi: 10.1029/2006GL027938.

[31] Peng, Z. G., and Y. Ben-Zion, (2006) Temporal changes of shallow seismic velocity around the Karadere-Duzce branch of the North anatolian fault and strong ground motion, *Pure Appl. Geophys., 163*, 567-600.